Wave phenomena in space plasmas

C. UBEROI
Department of Mathematics, Indian Institute of Science, Bangalore 560 012, India.

Abstract

Some aspects of the phenomena of proton whistlers, long-period micropulsations and microscopic structure of auroras are explained as manifestations of low-frequency wave processes in the magnetospheric plasmas.

Keywords: Wave phenomena, space plasmas, plasma waves, proton whistlers, magnetospheric plasmas, micropulsations.

1. Introduction

Only about forty years ago scientists began to understand the space around our planet Earth. We know that the Earth's atmosphere, extending up to 80 or 90 km, consists essentially of neutral gases. Above the height of about 100 km, ionized matter dominates the neutral form, as with increasing altitude the air becomes more and more ionized by ultraviolet light and X-rays from the Sun. The use of Saha's equations tells us that the matter will be ionized at these temperatures. The region from 100 km to about 1000 km is the ionosphere. For decades scientists believed that plasma density beyond the ionosphere decreases rapidly with increasing radial distance from the Earth. In this view, our planet and its magnetic field exist essentially in a vacuum. With the advent of the space age in 1957, spacecraft and rocket flights have changed this view drastically. Now we know that the Earth's magnetic field organizes the matter around the Earth in the form of an asymmetric cavity called the 'magnetosphere' (Fig. 1).

Before describing this picture, it is useful to explain briefly how the magnetosphere forms. The Sun's corona, which is a plasma with temperature above 10^6 K, escapes the Sun's gravity as it has too much energy, and streams away in the radially outward direction from the Sun. It also carries with it the Sun's magnetic field. This mixture of ions, electrons and magnetic fields is called the 'solar wind'. The solar wind moving typically with a velocity of 100 km/s or more sees our planet as an obstacle. Since it is a supersonic flow, it does not have the time to adjust itself to the obstacle and so it forms a 'shock', called the bow shock, about 14–16 Earth radii (R_E) away from the Earth. Across this shock the solar wind flows with lower velocities into a turbulent region called the magnetosheath. The other boundary where the solar wind pressure is balanced by the pressure exerted by the Earth's magnetic field marks the actual outer boundary of the magnetosphere and is called the magnetopause.
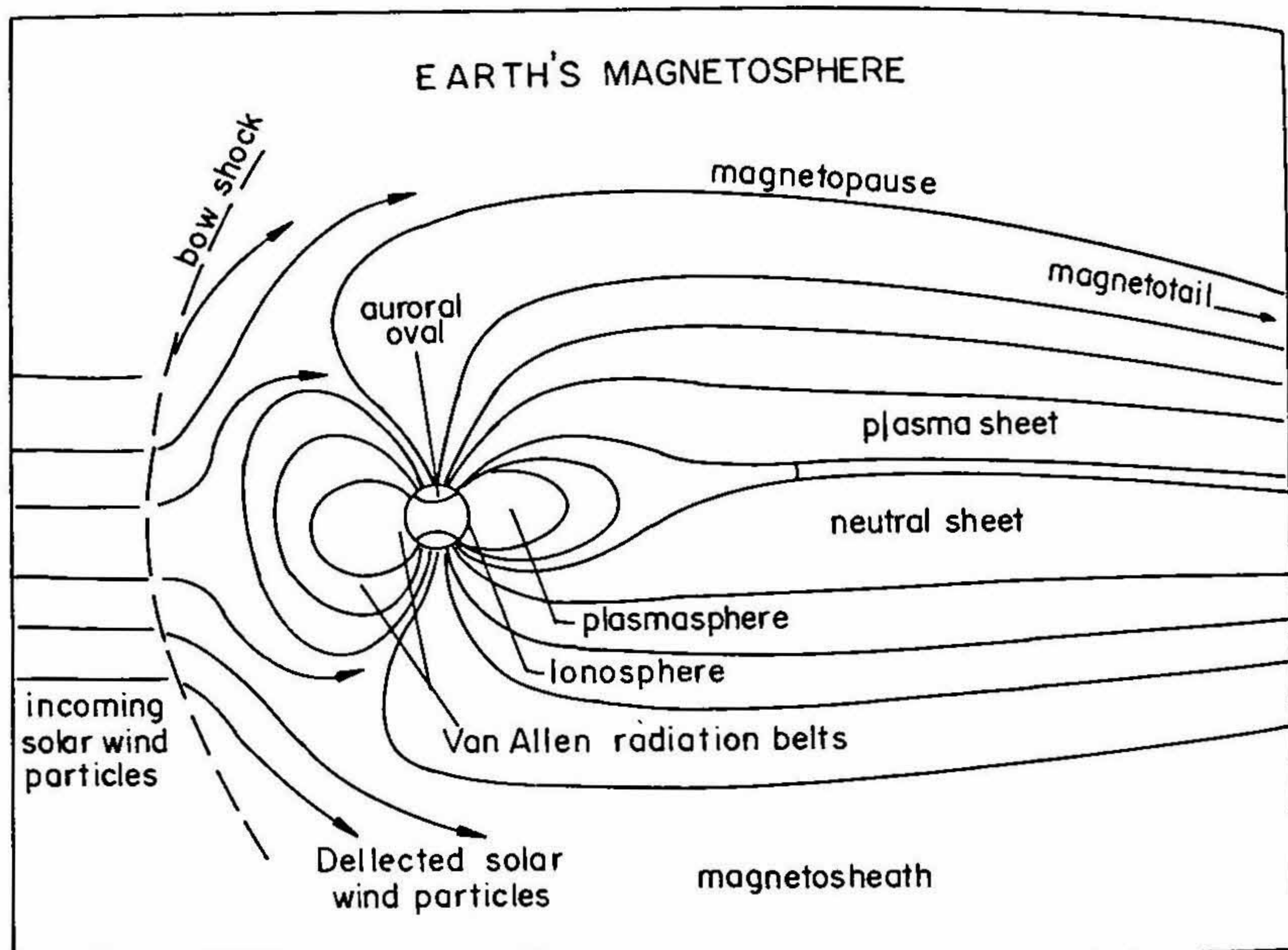
EARTH'S MAGNETOSPHERE

FIG. 1. The overall structure of Earth's magnetosphere.

The magnetosphere, as is seen in Fig. 1, approximates a closed cavity at $10-12 R_E$ on the side facing the Sun, but extends to more than $1000 R_E$ on the opposite side, or the midnight side, and is called the magnetotail. Since our moon is only $60 R_E$ away from us, it spends a week or so in the magnetotail each month. The other important regions are plasma sphere, neutral sheet and Van Allen belts of trapped electrons.

The various plasma regions with different densities and temperatures in the magnetosphere interact with each other and also with the very high energy charged particles in some areas. This makes the magnetosphere a very dynamic plasma system. Deriving energy from the Sun it can support various types of plasma waves and instabilities. Some very interesting natural phenomena which were a puzzle to scientists a few decades ago can now be explained as manifestations of wave processes in the magnetosphere.

This paper discusses the phenomena of 'whistlers', 'micropulsations' and 'aurora'. The choice of these topics is mainly due to the reason that as an applied mathematician I have been closely working with mathematical theories evolved to understand these phenomena. However, a little reflection about these topics led me to note that, since whistlers were first heard on the telegraphic receivers, micropulsations were first observed by the sensitive instruments known as magnetometers and auroras were discovered as a

dramatic visual spectacle in the sky, we are going to discuss the most fascinating 'light' and 'sound' show put up by Nature.

2. Whistlers

The earliest examples of recognized plasma waves received on the Earth were whistlers, the waves which actually whistle! In the early days of telegraphy, whistlers were heard on receivers connected to long wires, especially on stormy nights with plenty of thunder and lightning. It is not surprising that operators associated these with 'supernatural' forces from outer space! Some even associated them with people from Mars and some with flying saucers. Now we know mainly from the work done by Storey[1] that whistlers originate from lightning strokes in the atmosphere. Part of the bolts radioemission is refracted up through the ionosphere into the magnetosphere, where the energy is guided along the magnetic field lines. When the waves reach the magnetic 'conjugate' point in the opposite hemisphere, a portion is reflected back along the original path and a part refracted down to the ground. In this process electromagnetic waves of radiofrequency propagating in the plasma are dispersed. The dispersion relation for waves propagating in a 'cold' plasma (when thermal effects are not important) at an angle θ to the magnetic field direction is given as[2]

$$An^4 - Bn^2 + C = 0, \tag{1}$$

where

$$A = S \sin^2 \theta + P \cos^2 \theta, \quad B = RL \sin^2 \theta + PS(1 + \cos^2 \theta),$$

$$C = RLP,$$

$$R = 1 - \sum_k \frac{\omega_{pk}^2}{\omega(\omega + \varepsilon_k \omega_{ck})}, \quad L = 1 - \sum_k \frac{\omega_{pk}^2}{\omega(\omega + \varepsilon_k \omega_{ck})},$$

$$P = 1 - \sum_k \frac{\omega_{pk}^2}{\omega^2}, \quad S = \frac{1}{2}(R + L), \quad D = \frac{1}{2}(R - L).$$

Here $\varepsilon_k = q_k / |q_k|$, with k summed over all charged particle species in the plasma, ω_{ck} is the gyrofrequency, ω_{pk}, the plasma frequency and q is the charge.

For whistlers, or more precisely electron whistlers, making a distinction for subsequent discussions, ions do not play an important role. As whistlers propagate along the magnetic lines of force, $\theta = 0°$. The refractive index of whistlers, therefore, becomes

$$n_R^2 \equiv \frac{c^2 k^2}{\omega^2} = 1 - \frac{\omega_{pk}^2}{\omega(\omega - \omega_{ce})}. \tag{2}$$

For $\omega \ll \omega_{ce}$, $k \propto \sqrt{\omega}$, which gives group velocity $v_g = \partial \omega / \partial k \propto \sqrt{\omega}$.

The group time delay, therefore, is

$$t = \int \frac{ds}{v_g} \alpha \frac{1}{\sqrt{\omega}} \, .$$

(3)

This dispersion, therefore, makes the higher frequencies reach the receiving station before the lower ones, producing a characteristic 'whistle' that drops rapidly in pitch on an audio receiver. Within one second, a whistler that has an initial frequency as high as 15,000–30,000 Hz reaches about 1000 (Fig. 2).

There are different types of whistlers, not only depending on the type of classified sound associated with these but also on the number of reflections from conjugate points. A whistler which has crossed the equator once is known as a one-hop whistler, and that which has crossed twice, two-hop, and so on. A ground station will see a whistler when it has crossed the equator at least once. A satellite, on the other hand, can pick up a whistler which is yet to reach the equator. These whistlers are called fractional-hop whistlers. I shall now discuss an interesting phenomenon associated with the fractional-hop whistlers arising in the study of waves in multicomponent plasmas[3].

2.1. Proton whistlers

In 1963–64 the VLF recording from the satellites Alouette I and Injun III showed an unusual VLF phenomenon associated with the propagation of whistlers in the ionosphere. The satellites were at a height of 1000 and 1800 km, respectively. This new effect appeared on the frequency–time spectrogram obtained from the observations as a tone which starts immediately after the reception of a short fractional-hop whistler at the satellite. This tone initially shows a rapid rise in frequency and then reaches a very nearly constant value. It is an ascending tone rather than the descending one heard with the whistlers. The tone started at frequencies much below 1 kHz. Similar recordings from both the satellites ensured that the tone was not due to some interference from the equipment in the satellite. The constant frequency was 520 Hz for Alouette I and 400 Hz for Injun III. These frequencies were the proton gyrofrequencies of the plasma in the vicinity of the satellite. Gurnett et al.[4], the scientists who first observed this phenomenon, called this ascending tone as 'proton whistler', and now in general this is known as ion whistlers: whistlers because the source was the energy from the lightning discharge, and ion because the maximum frequency reached is the ion gyrofrequency instead of the electron gyrofrequency (Fig. 2).
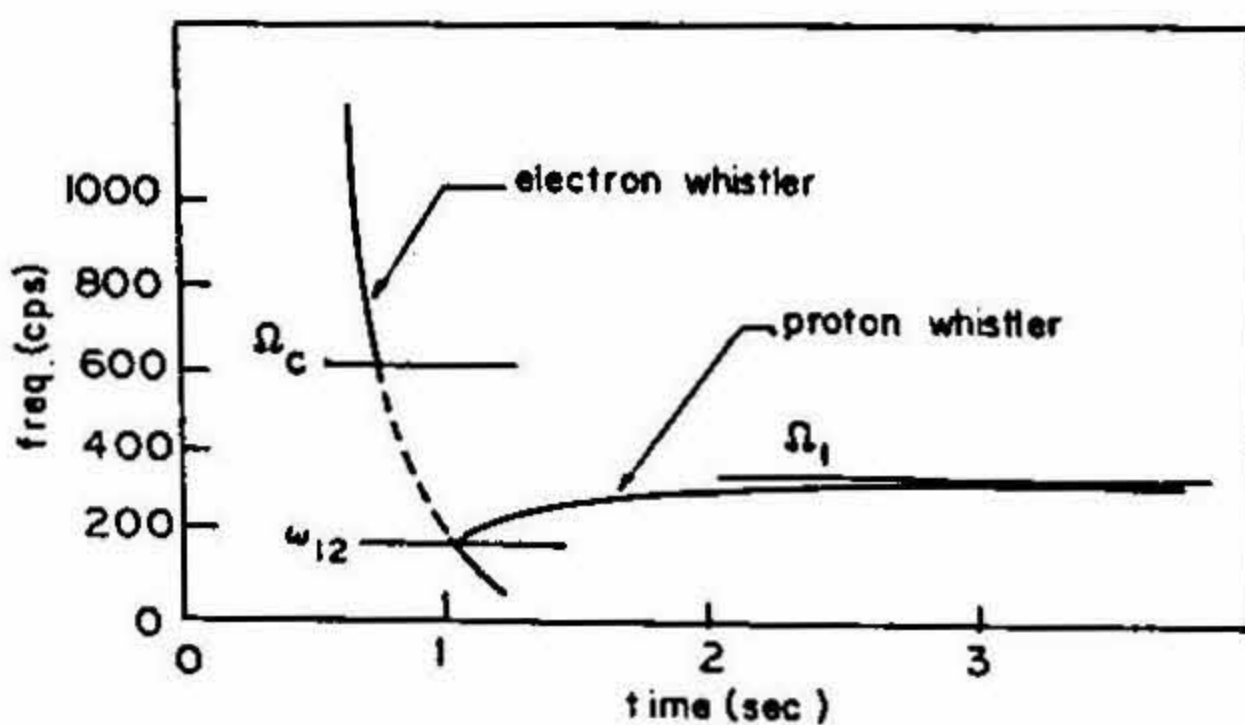

FIG. 2. Spectrogram showing a proton whistler and the nomenclature.

To explain the proton whistler phenomenon on the basis of wave propagation theory, we have to consider the effect of ions in eqn (1). The roots of eqn (1) will be given as

$$n_{1,2}^2 = \frac{B \pm \sqrt{B^2 - 4AC}}{2A}.$$ (4)

For $n_1^2 = n_2^2$, $B^2 - 4AC = 0$, which gives

$$(RL - PS)^2 \sin^4 \theta + 4P^2D^2 \cos^2 \theta = 0.$$ (5)

For $\theta = 0$, this condition is satisfied for $PD = 0$; $P = 0$ is a singular case, so we have $D = 0$. The roots of $D = 0$ can be checked to exist only when the plasma has more than one ion species. The values at which $n_1 = n_2$ are called cross-over frequencies; for a two-ion plasma, this frequency lies in the propagating band between the gyrofrequencies of the ions. The generalization to n-component plasma consisting of only positive ions is straightforward but, as we shall see, this is not true when the plasma consists of negative ions.

The wave polarization coefficient ρ for these waves is

$$\rho = \frac{iDn^2 \cos \theta}{Sn^2 - RL}.$$ (6)

It is seen that $\rho_1 \rho_2 = 1$ and so when $n_1 = n_2$, at those frequencies $\rho_1 = \rho_2 = \pm 1$. The wave polarization ρ becomes a function of position during propagation in nonuniform plasma and can pass through a region where coupling phenomenon occurs. Coupling here means that when a wave of one type is incident on a coupling region, generally speaking, waves of two types leave it. It other words, in this region there occurs a partial change of waves of one type into another, which is accompanied by a significant alteration in the polarization of the wave.

The coupling parameter ψ is defined by Forsterling (see Budden[5]) as

$$\psi = \frac{1}{2k_0} \frac{d\rho_1}{dz} \frac{1}{(\rho_1^2 - 1)}$$

$$= \frac{1}{2k_0} \frac{d\rho_2}{dz} \frac{1}{(\rho_2^2 - 1)}, \quad \rho_1 \rho_2 = 1.$$ (7)

When $\theta = 0$, $D = 0$, $\rho = \pm 1$; hence, across $D = 0$ we have the critical coupling condition.

The fractional-hop whistler which is a right-circularly polarized wave drops down in frequency much below the electron gyrofrequency while propagating in the inhomogeneous magnetospheric plasma along the magnetic field direction and meets the cross-over frequency ω_{cr}. Across ω_{cr}, the polarization changes and the right-hand-polarized wave emerges as a left-hand-polarized wave. This is the ion cyclotron wave which has a resonance ($n_L^2 = \infty$) at $\omega = \omega_{ci}$. The ion cyclotron whistler reaches the resonant frequency, the ion gyrofrequency, as the maximum value. Thus, the dispersion due to the
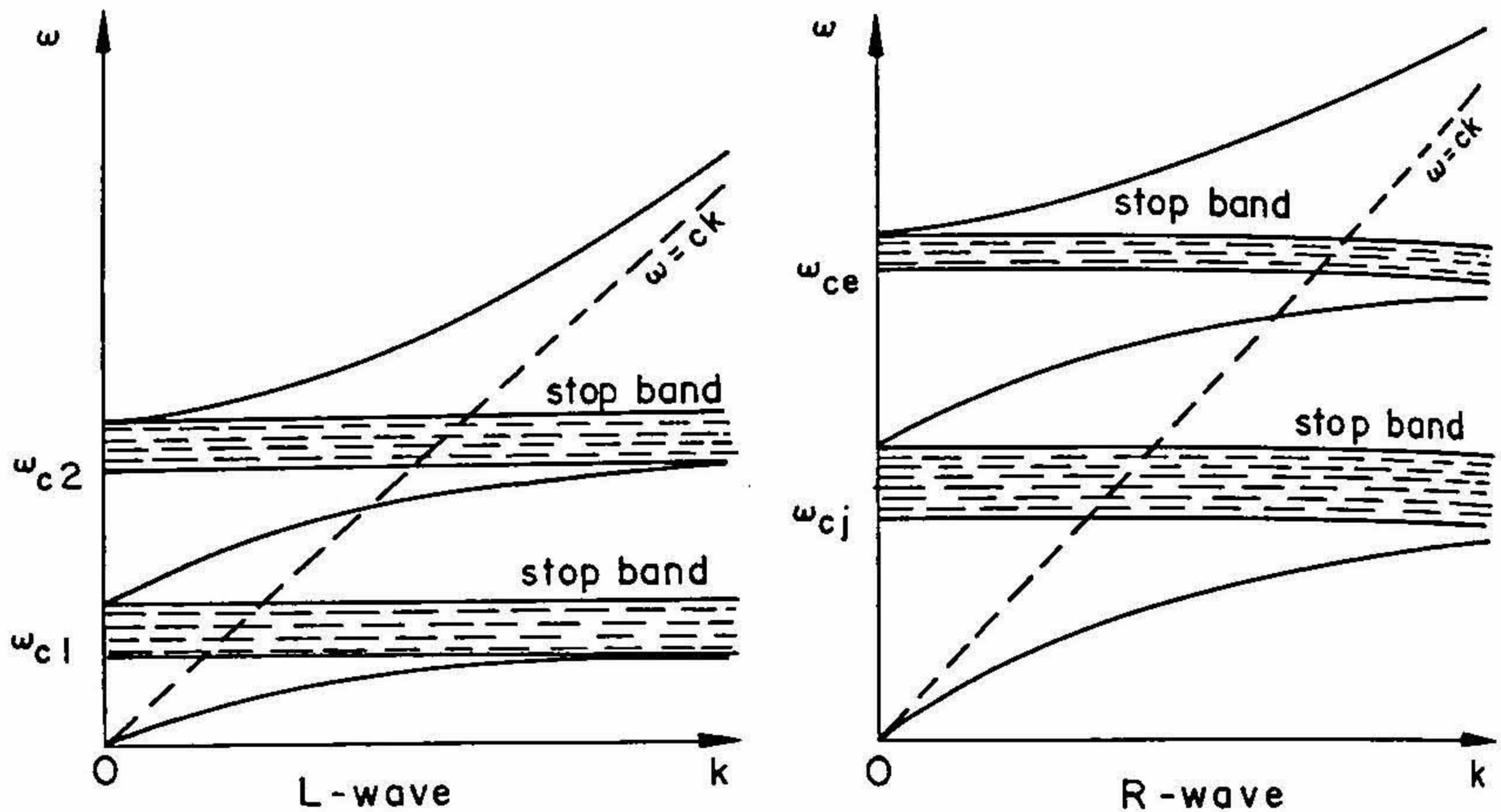
FIG. 3. Dispersion diagrams of left- and right-circularly polarized waves for plasma consisting of two positive and one negative ion species.

presence of two or more types of ions gives rise to ion whistlers which are a descending tone. The ion whistlers propagate far into the magnetospheric plasma, providing an important means of measuring the ion densities and temperatures of plasmas in these distant regions.

The plasma can have both positive and negative ions. A multicomponent plasma with negative ions was considered by Uberoi and Das[6] to understand the formation of negative-ion whistlers and thus find a way to measure the plasma parameters related to the population of negative ions. But it was found that as the negative ions introduce pass and stop bands in the right-circularly polarized wave also (Fig. 3), the existence and behaviour of the cross-over frequencies becomes more complex compared to positive-ion multicomponent plasmas. Hence, the formation of negative-ion whistlers and the applications of these for measuring the negative-ion densities and temperatures as suggested by Shawhan[7] can present some difficulties. This point was discussed in detail for a simple model of plasma with two positive ions and one negative-ion species by Das and Uberoi[8]. A generalization to plasmas with any number of positive and negative ions was given by Uberoi[9].

3. Micropulsations

3.1. *Introduction*

The Earth's magnetic field intensity is now known to vary on a variety of time scales ranging from periods of millions of years to fractions of a second. Only the variations which are now known as geomagnetic micropulsations are discussed here. These pulsations are relatively fast, low-amplitude changes that typically have periods ranging from

a few minutes to fractions of a second and amplitudes of a few orders of nT (nano-Tesla).

These rapid changes in the Earth's field have been measured with magnetometers placed on the Earth's surface and, in the last two decades, on Earth-orbiting and interplanetary spacecrafts. The first observations of a few minute time variations of the Earth's field were reported in 1859; thus, the existence of few minute variations in the Earth's field has been known for over a hundred years. Nevertheless, the great impetus for the micropulsation study came during the International Geophysical Year 1957–58. These studies ultimately led to the classification of geomagnetic pulsations into categories according to the frequency of the variations and characteristic features (continuous or irregular) as Pc 1-5 and Pi 1-2.

The suggestion that the hydromagnetic waves in the magnetosphere were a likely source of geomagnetic pulsations was first made by Dungey[10] in 1953. Now we know that the low-frequency hydromagnetic waves are a common feature of space plasmas. Many a phenomena in solar atmosphere or heliosphere, planetary and cometary magnetospheres can be related as a manifestation of the linear or nonlinear Alfvén waves. Considering only the linear theories, an important and somewhat amazing phenomenon of Alfvén waves is the resonant mode coupling to surface or global modes of an inhomogeneous plasma[11]. As inhomogeneity is an important characteristic feature of the various regions of space plasmas, the resonant mechanism of Alfvén waves finds applications in modelling and understanding of phenomena like ULF waves or micropulsations, substorms, magnetosphere–ionosphere coupling, aurora formations field-aligned currents and charged-particle acceleration in planetary magnetospheres and in understanding of physics of the outer heliosphere. Keeping in view my own current interest, I would like to give a brief review of the recent developments in the study of resonant mode coupling theories with a view to understand the time-dependent theories of micropulsations.

3.2. Steady-state theories

The theoretical understanding of the origin and the characteristic properties of ULF hydromagnetic waves or micropulsations (ranging from above 1 mHz to the local proton gyrofrequency ~ 1 Hz) in planetary magnetospheres has shown that most pulsations with a long period (> 10 s in the Earth's magnetosphere) are generally believed to be field line oscillations (Fig. 4) excited by the external and internal source waves through the linear resonance mechanism. Due to the strong factor of inhomogeneity, the standing Alfvén mode frequencies vary from magnetic shell to shell and purely transverse signals are highly localized to particular shells. Field line resonance is a descriptive term for these purely localized signals along the magnetic field lines of the Earth's dipole magnetic field.

Basically, the understanding of resonant mode coupling translates into the mathematical problem of analysis of the hydromagnetic wave equation in inhomogeneous magnetic fields and the density. Here we shall consider the variation in the planes perpendicular to the magnetic field direction. There is a considerable interest in the study of
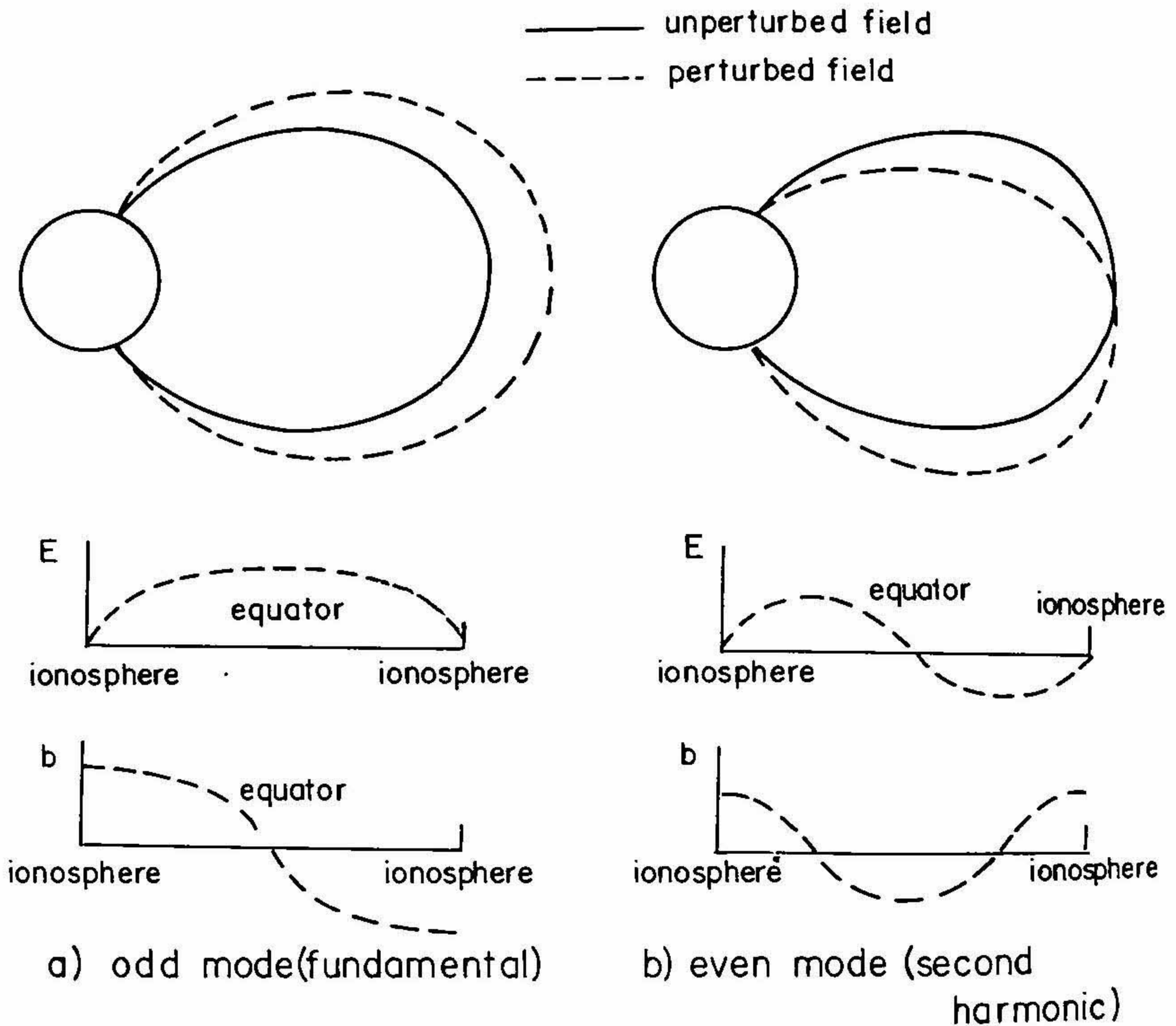
FIG. 4. Schematic picture on two lowest-frequency modes of standing oscillations on a field line, assuming perfectly conducting ionospheres. E and b are electric and magnetic field perturbations.

resonance mechanism in two-dimensional systems and it is seen that the basic concepts of resonant coupling theory hold good even in these systems[12].

The normal mode analysis[13] of the hydromagnetic wave equation or the steady-state theories of ULF waves in the magnetosphere showed that when a monochromatic source with frequency ω_0 is present in the magnetosphere, magnetic pulsations can be excited at the frequency of the source, with the intensity maximum at an L-shell value of the resonant field line, where the Alfvén resonant condition $\omega_0 = k_{11}(L)V_A(L)$ is satisfied. Here $k_{11}(L)$ is the wave number parallel to the magnetic field direction and $V_A(L)$ is the Alfvén velocity at the L-shell. These theories have successfully explained a majority of ground and spacecraft measurements, in which the same frequency is observed at different latitudes for a given event, with variations in the polarization and amplitude.

The linear resonance theory, though very successful, has some shortcomings which have been pointed out in the literature from time to time; some were not valid and some
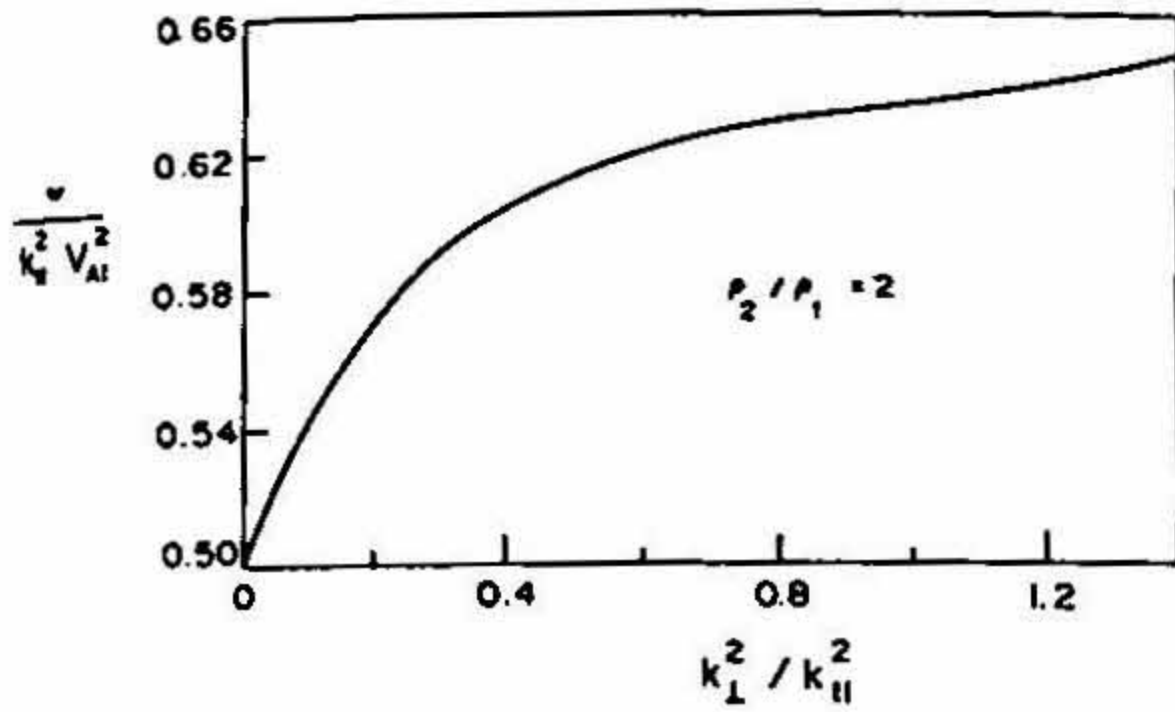
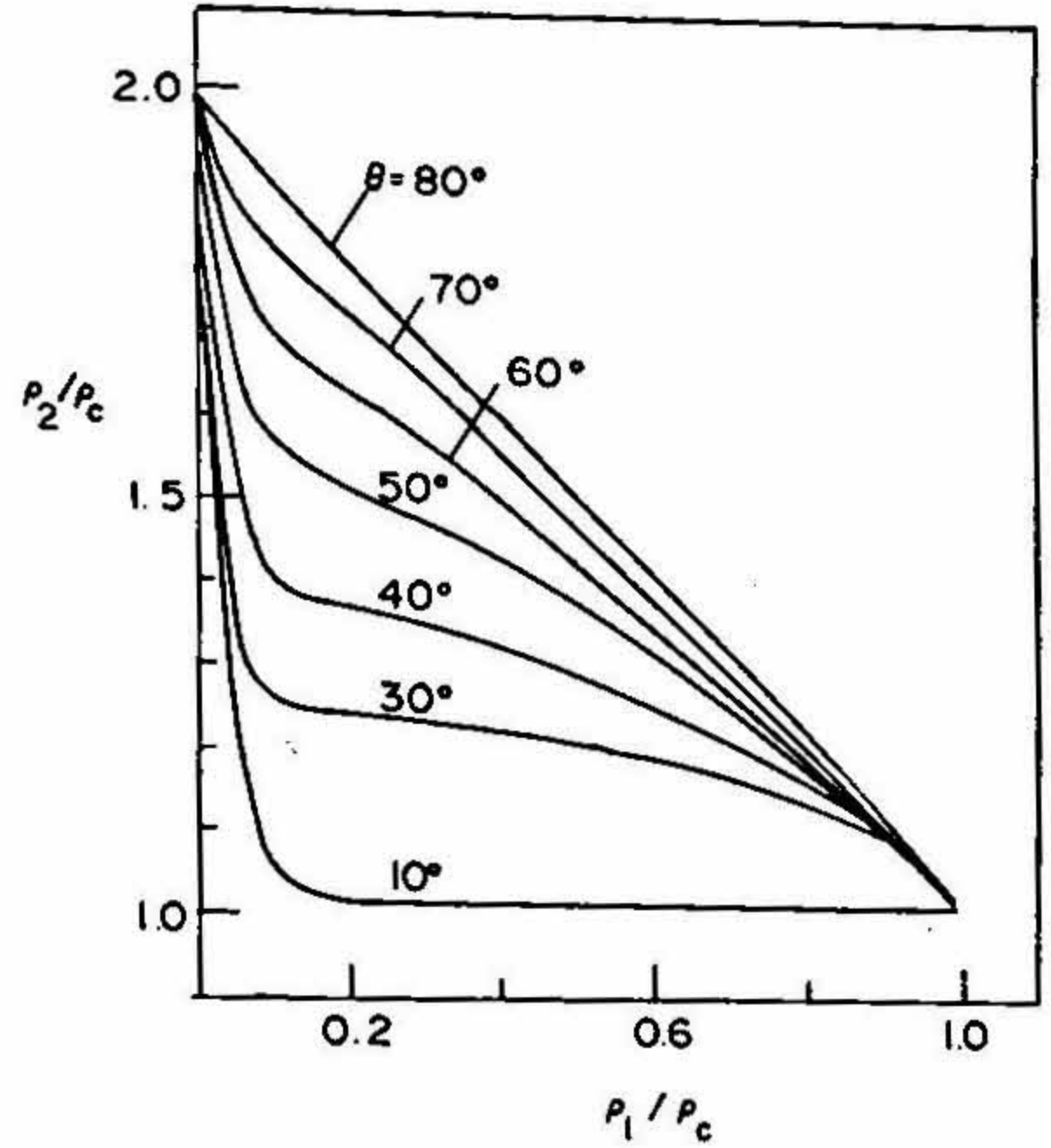FIG. 5. Dispersion curve for the Alfvén compressional surface wave.

FIG. 6. The parametric analysis of the dispersion equation gives the relationship between the densities on either side of the discontinuous surface required for the existence of Alfvén compressional surface waves.

needed attention. The criticism pointed out by Yumoto and Saito[14] was that the resonance coupling between the surface waves excited at the magnetopause and the standing wave oscillations never occurs in the magnetosphere. This was shown to be invalid as
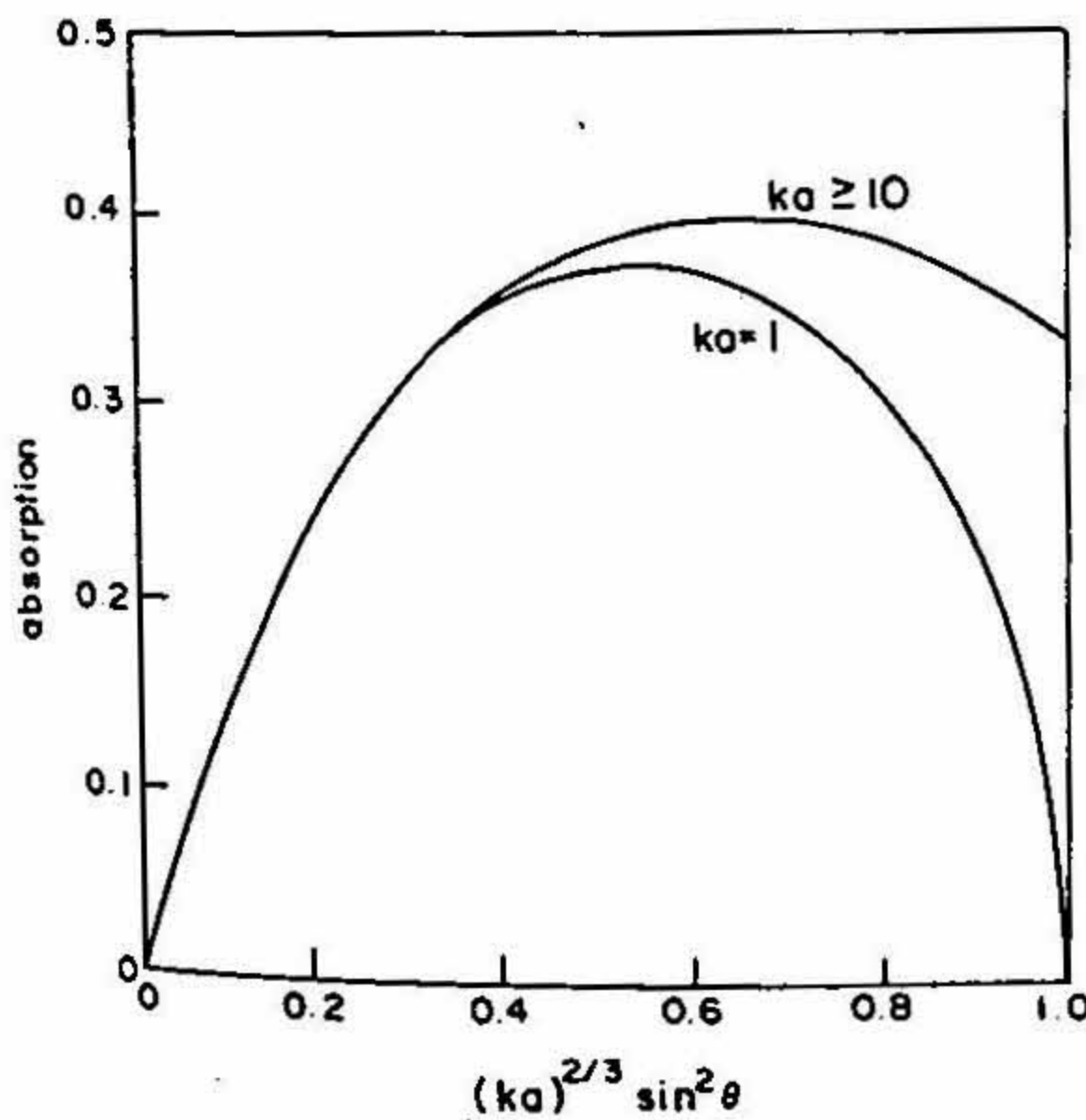
FIG. 7. Power absorption coefficient as a function of wave number k and the angle of propagation. $2a$ is the scale length of the density variation.

Uberoi[15] pointed out that the ω_0 for the surface waves was not calculated correctly. The correct value of ω_0 matched very well with the field line oscillations calculated for different values of L and propagation along θ in the work by these authors. The other major shortcoming is that the steady-state theory studies the resonant mode coupling and resonant absorption only for $k_{11} \ll k_{\perp}$, i.e., for large azimuthal numbers. Uberoi[16] has shown that if this assumption is not considered, the characteristic properties of compressional surface waves and the mechanism of resonant absorption differ considerably (Figs 5-7). This needs to be looked into more seriously.

Recently, Uberoi[17] has shown that though the mathematical analysis of the Alfvén wave equation does not show any variation at the nonzero or the zero singular point, the role of surface waves in the physical mechanism of resonant absorption of Alfvén waves is very much different at these points. This requires a certain modification in the linear resonance theory while considering resonant mode coupling near the neutral point. The difference becomes all the more emphasized when resistivity is taken into account. At the neutral point the zero-frequency surface waves ($ka \ll 1$), which are symmetrical surface modes of the structural neutral layer, couple to the tearing mode of instability of the layer. This result can be very important in the study of energy balance in tearing modes and the association of surface waves to driven magnetic reconnection.

Can these zero-frequency surface waves occur along the magnetopause? To answer this take $ka = 10^{-2}$, the Alfvén speed 300 km/s and the neutral layer thickness a varying from 100 to 300 km. This gives frequencies ranging from 3×10^{-2} to 0.9×10^{-2} Hz
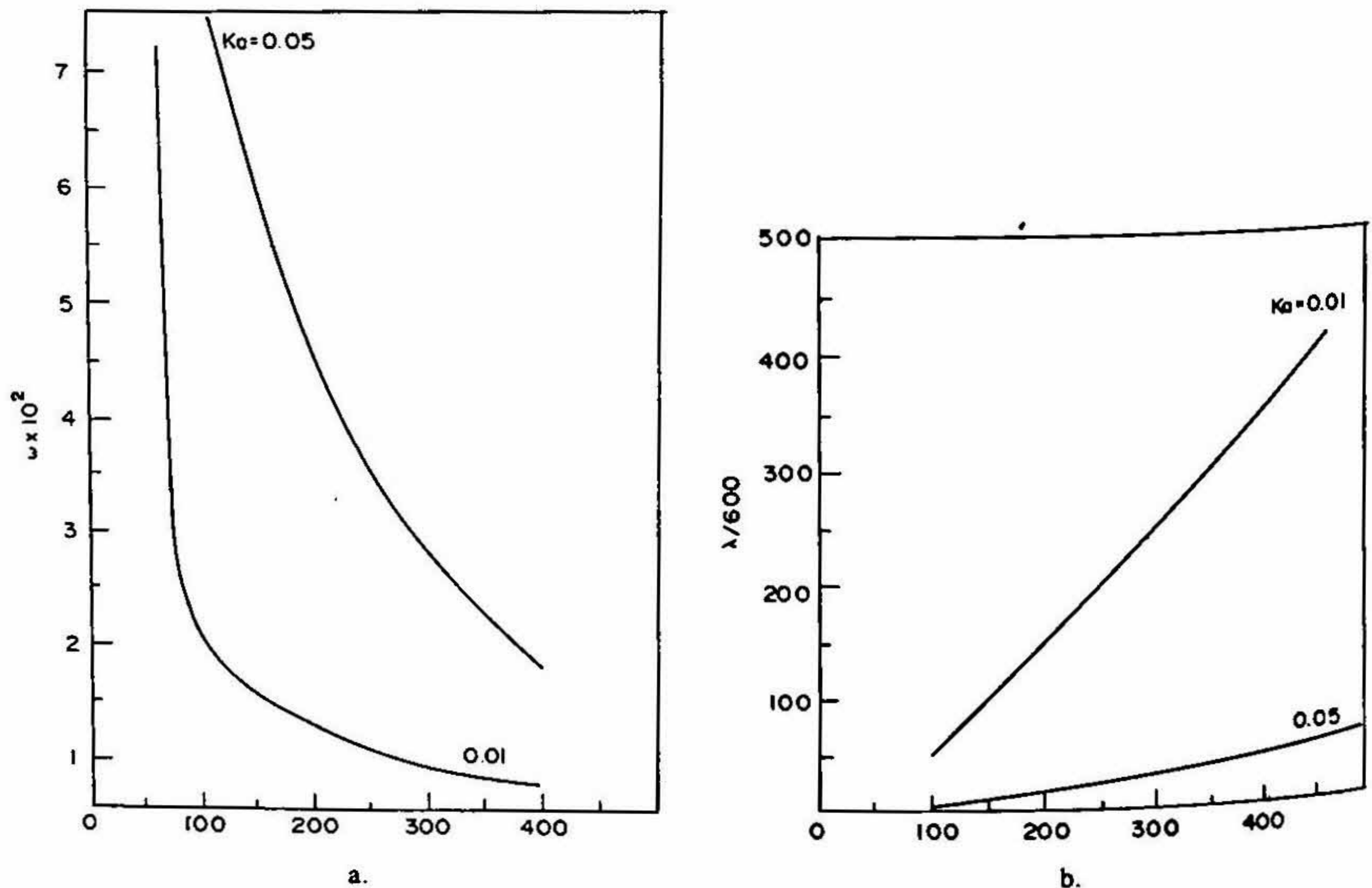

FIG. 8. Variation of frequency and wavelength with a, the thickness of the neutral layer.

(Fig. 8). The time periods vary from 3 to 6 min. The surface waves with periods greater than 2 min have been observed along the magnetopause. Therefore, it appears that the zero-frequency surface waves can be an important mechanism for inducing tearing instability, which has been suggested to occur at the dayside magnetopause, and consequently these waves could be an important driving mechanism for magnetic reconnection[18].

The steady-state linear resonance theory obviously cannot explain the features of micropulsations, which are a manifestation of the temporal behaviour of the hydromagnetic waves excited by time-dependent sources. Although a few studies were made earlier to look at the asymptotic behaviour of the solutions of the hydromagnetic equation resulting from impulsive stimulus of the magnetospheric system, the need for proper time-dependent theories of this equation has been realized recently. In the next section this subject is reviewed briefly.

3.3. Time-dependent theories

Hasegawa et al.[19] extended the steady-state approach to include a particular case of broad-band source in their analysis to explain the earlier reports of ground-based observations of pulsations whose period is a function of magnetic latitude for the same event. Recent spacecraft and multipoint ground-based observations have increased the understanding of both external and internal sources of generation of ULF waves. It is now understood that ULF waves can be generated by impulse excitation of the magnetosphere due to solar-wind–magnetosphere interaction, flux transfer events and sudden compression of the magnetosphere due to interplanetary shock. Further, the presence of such broad-band impulsive sources led to a puzzle as to why these sources of energy should lead to the almost monochromatic waves that are often observed. This led to the proposal of the global mode oscillations of magnetospheric cavity in the presence of an external stimulus by Kivelson and Southwood[20] (see also Uberoi[21]). The magnetosphere reverbrates with the natural fast modes of the magnetospheric cavity formed by the magnetopause and the turning point arising due to the gradient in the Alfvén velocity. The impulse-excited hydromagnetic narrow-band global cavity modes, stimulated by broad-band solar-wind disturbances, coupling to field line resonances in the magnetosphere has become a topic of great interest. Various numerical models have been developed[22–25] to study the time development of impulse-excited hydromagnetic cavity and field line oscillations in a sheared magnetospheric plasma considering particular types of impulse stimulus at the magnetopause. The possibility of such excitations has been proved to exist but substantial evidence showing the existence of cavity modes in the magnetosphere is still due. Also, the observed frequencies seen by the Johns Hopkins University/Applied Physics Laboratory (JAU/APL) radar of the field line resonances are much lower than those predicted by the cavity model. This gave rise to the concept of MHD waveguide model, treating the magnetosphere as an open waveguide[26]. The cavity here is now extended towards the magnetotail to form the waveguide configuration. Dispersion and wave coupling in inhomogeneous waveguides has recently been studied by Wright[27]. Based on certain observations of standing waves, Harrold and Samson[28] extended the waveguide model, suggesting that the bow shock rather than the magnetopause must be

taken as the outer boundary of the cavity/waveguide. This model is referred to as the standing ULF waveguide model.

It is now understood that field line reasonances can be driven by impulse-excited surface, cavity, waveguide, and standing ULF waveguide eigenmodes. In all these cases it is necessary to understand the features of impulse-excited field line oscillations for a general class of initial impulse stimulus at the magnetopause. Most of the theoretical work referred to above considered a particular boundary or initial perturbations while studying the solutions of hydromagnetic equation. Recently, Uberoi[29] and Uberoi and Sedlacek[30] have considered the time-dependent solution of the Alfvén wave equation for a general class of initial conditions. Using these solutions, features of free oscillations of field lines are studied in detail[31]. Some of the important results are discussed briefly in the following section.

3.4. *Impulse excitation of field line oscillations*

We start with the well-known Alfvén wave equation given as (for example, see Uberoi[11])

$$\nabla \cdot \left[\left\{ \frac{\partial^2}{\partial t^2} - \frac{1}{4\pi\rho_0} (B_0 \cdot \nabla)^2 \right\} \nabla v_x \right] = 0, \tag{8}$$

where v_x is the x-component of the velocity field, and the equilibrium magnetic field variation given as

$$B_0(x) = B_{0y}(x)\, \hat{y} + B_{0z}(x)\, \hat{z}. \tag{9}$$

Fourier analysis of eqn (1) with the space dependence $\exp[i(k_y\, y + k_z\, z)]$ gives

$$\frac{\partial}{\partial x} \left[\left(\frac{\partial^2}{\partial t^2} + \omega_A^2(x) \right) \frac{\partial v_x}{\partial x} \right] - k^2 \left(\frac{\partial^2}{\partial t^2} + \omega_A^2(x) \right) v_x = 0, \tag{10}$$

where $k^2 = k_y^2 + k_z^2$ and $\omega_A^2(x) = [B_0(x) \cdot k]^2 / 4\pi\rho_0$.

Following Uberoi and Sedlacek[30] the integrodifferential formulation of eqn (10) can be written as

$$\left(\frac{\partial^2}{\partial x^2} - k^2 \right) \left(\frac{\partial^2}{\partial t^2} + \omega_A^2(x) \right) \frac{\partial e_k(x, t)}{\partial x} = \underbrace{k^2 \frac{\partial \omega_A^2(x)}{\partial x} \int_{-\infty}^{x} e_k(s, t)\, ds}_{\text{coupling terms}}, \tag{11}$$

where $e_k(x, t) = \partial v_x / \partial x$. The coupling of surface waves to the local Alfvén oscillations on the left-hand side of eqn (11) is seen to arise due to inhomogeneous Alfvén frequency $\omega_A(x)$ on the right-hand side of this equation.

The time-dependent solution of eqn (11) for the boundary conditions $e_k(x, t) \to 0$ as $|x| \to \infty$ and initial conditions

$$e_k(x, t)]_{t=0} = \phi(x, k) \quad \text{and} \quad \frac{\partial e_k}{\partial t}(x, t)\Big]_{t=0} = \psi(x, k), \tag{12}$$

where $|\phi(x, k)|$ and $|\psi(x, k)| \to 0$ as $|x| \to 0$, has been obtained as

$$e_k(x, t) = \frac{\partial v_x}{\partial x} = \phi(x, k)\cos[t\omega_A(x)] + \psi(x, k)\frac{\sin[t\omega_A(x)]}{\omega_A(x)}$$

$$+ \int_0^t \frac{\sin[\omega_A(x)(t-\tau)]}{\omega_A(x)} K(x, \tau, k)\, d\tau, \tag{13}$$

where $K(x, \tau, k)$ is a convergent series of operators on $e_{k0}(x, t)$, which represent the first two terms of the solution in eqn (13).

Let us now examine the impulse response of the incompressible, inhomogeneous magnetospheric plasma to surface-wave-like impulse excitations at the magnetopause. This will then give the time development of the field line resonances. As we are looking only at the free oscillation problem, the first two terms in the solution (12) are taken to find the various field quantities for initial conditions (11). Calculations of v_x, v_y, vorticity component $(\text{curl } v)_z$ and current density J_z allow us to arrive at the following results:

1. For a general initial perturbation of the type (11) the impulse response of the magnetosphere showed the ringing of field line at the Alfvén frequency, with amplitude decaying as $1/t$ from the initial value.

   We also note that the v_y component, along the magnetic field, does not show decay with time whereas v_x decays as $1/t$. Hence, eventually for large t the wave becomes a longitudinal wave.

2. The expressions for the components of vorticity and current density were found to have secular terms with t. Thus, both these physical quantities showed increase with time t, reminiscent of a collisionless system driven at its resonant frequency. From the vorticity/current density expression we get the phase-mixing time as

$$t_{ph} = \frac{k\omega_{A0}(x)}{\phi(x_0, k)} \frac{1}{d\omega_A/dx}, \tag{14}$$

where $x = x_0$ is an initial point. For a magnetosphere with a magnetic field profile

$$B_0(x) = \frac{B_0}{1 + x^2/x_0^2}, \tag{15}$$

$x = 0$ corresponds to the equator and $x > x_0$ to the magnetopause.

In terms of the Alfvén transit time N_c, we get

$$N_c = \frac{\omega_{A0}^2}{2\pi} \frac{k}{\phi(x, k)} \frac{1}{d\omega_A/dx}. \tag{16}$$

Considering $V_{A0} = 600$ km/s at $x = x_0$ and taking the impulse amplitude $\phi(x_0, k)/k \approx 1$ we have $N_c = 138\, kx_0$ for the profile (15). For the nondimensional wave number $kx_0 = 3$, $N_c = 414$. In general, for values $1 < kx_0 < 6$, the number of Alfvén oscillations is of the order 10^2. There should, therefore, be a good opportunity to observe ringing for time of the order of tens of Alfvén transit periods near the region $x = 0.5x_0$. We note that the number N_c increases with increase in the initial impulse amplitude.

3. The variable eigenperiods of the field line oscillations are given as $T = 2\pi / \omega_A(x)$ with

$$\omega_A(x) = V_A(x) \cdot k = V_A(x)\frac{n\pi}{l},$$

where l is the length of the field line. Taking a particular example: $V_A = 1250$ km/s at $x = 0.56$ and $L = 6.6$, for which field line length $l = 5R_E$, we get the time period for the fundamental mode as

$$T = \frac{2\pi l}{V_A \pi} = \frac{2l}{V_A} = \frac{2 \times 600 \times 5}{125} = 124 \text{ s.}$$

The order of eigenperiods of free oscillations can be seen to vary from tens to hundreds of seconds.

Allan et al.[22], considering the coupling of cavity and field line resonances, have given detailed numerical results showing the spatial and temporal structures of field line resonances using a cylindrical model. The features of ringing of field lines, phase mixing and variation of oscillation frequencies with latitude as obtained from the analysis of the solution (13) agree qualitatively very well with this numerical model. Finally, we would like to mention that the linear growth of current density with time was pointed out as early as 1974 by Radoski[32] for the toroidal (shear) mode in his study of the asymptotic temporal behaviour of hydromagnetic waves; no attempt, however, was made to discuss the phase-mixing phenomena.

3.5. Transient amplification of shear Alfvén waves

We shall now discuss the initial conditions for which a surface 'wavelet' when superposed on the sheared magnetospheric plasma shows the initial transient amplification, by using the solutions in eqn (13). These types of surface wavelets are caused by the passage of an interplanetary shock wave and have been observed[33] travelling tailward, by the satellite GEOS2. They are also important for fusion plasmas.

Consider the initial disturbance (12) of the type

$$\phi(x, k) = Ae^{-k|x|} e^{iu_0 kx}, \quad \psi(x, k) = 0, \tag{17}$$

with A as a constant.

Taking a linear Alfvén speed profile

$$V_A(x) = V_A\left(\hat{z} + \frac{x}{d}\hat{y}\right) \qquad (18)$$

with (17) and (18), eqn (13) with zeroth-order terms and $k_y \gg k_z$ on integrating gives

$$v_x(x, y, z, t) = \frac{1+u_0^2}{1+\left(u_0 - \dfrac{V_A t}{d}\right)^2} e^{-k|x|} \exp\left[ik_y x\left(u_0 - \frac{V_A t}{d}\right) + ik_z\left(z - \frac{V_A t}{d}\right) + ik_y y\right] + D. \quad (19)$$

Here $A = 2(1 + u_0^2)k$ and D is the part of the solution which does not show any amplification.

The solution (19) shows that for $u_0 > 0$ the amplitude of v_x increases from its initial value to a large amplitude till $t = du_0/V_A \equiv T$. For $t > T$, the amplitude decays and tends to zero for $t \to \infty$. Considering the quantitative values for magnetospheric region close to the geomagnetic equator, $v_A = 1000$ km/s and taking $d = 1 R_E$, we get $t = 6.4u_0$. Choosing $u_0 = 25$, which means that the inclination $k_x/k_y \gg 1$, we get $T = 160$ s. The wave amplification will be maximum at time $t = 160$ s; after $t = 2T = 320$ s, the wave begins to turn and start moving towards the resonant layer[35] (Fig. 9). These quantitative results agreed very well with the observations.

4. Kinetic Alfvén wave: Microscopic structure of auroras

4.1. Introduction

The study of the coupling of surface and the shear Alfvén waves by initial value problems indicates that in the process of resonant coupling the surface wave energy is being absorbed by the shear Alfvén waves. This energy is localized near the resonant surface
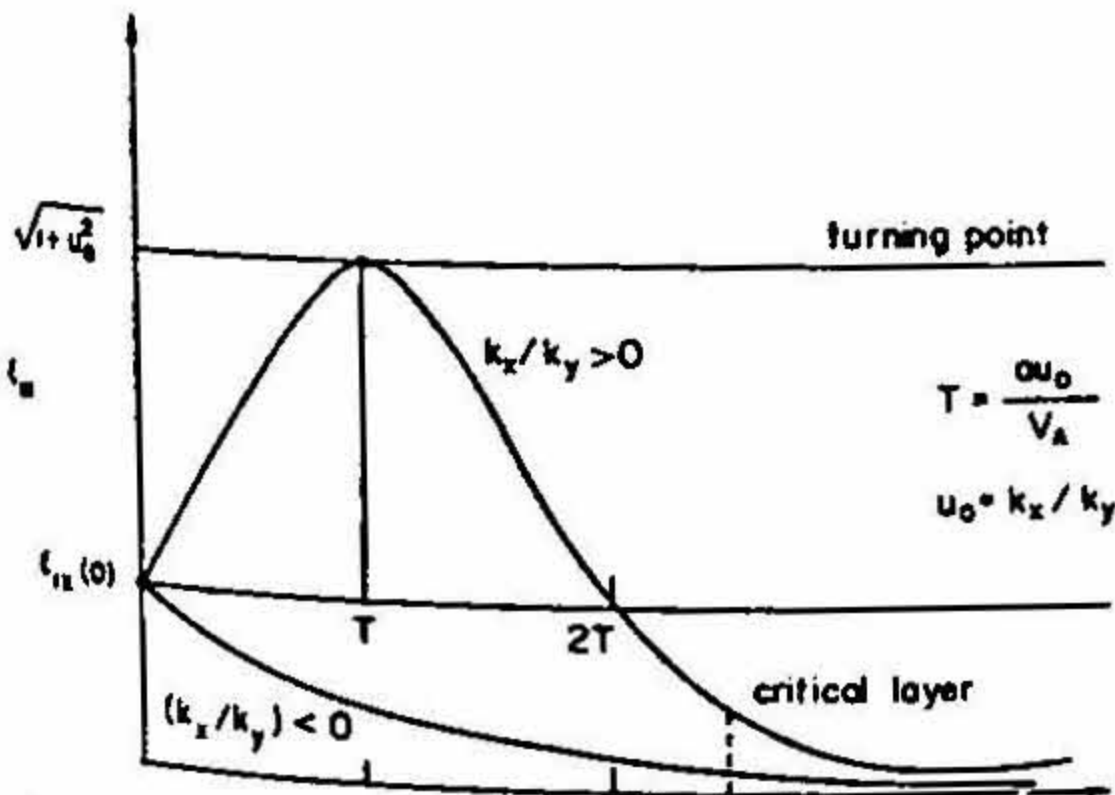

FIG. 9. A schematic sketch of the displacement vector in the x direction (perpendicular to the magnetopause) of the surface wavelet with time t both when the initial inclination $k_x/k_y > 0$ and when $k_x/k_y < 0$.

in the ideal MHD system. When collision effects like viscosity, finite conductivity or microscopic effects are taken into account, the singularity of the differential equation disappears, in the sense that the equation becomes a fourth-order differential equation and the singularity remains in the perturbation sense. In this case the shear Alfvén wave has a discrete spectrum but the dispersion relation is modified due to collisional or microscopic effects. The localized energy is therefore propagated away by the Alfvén wave, which is now damped by the collisional effects or in the microscopic case by collisionless Landau damping, thus depositing the surface wave energy into the plasma[13].

The energetics of the resonant absorption of Alfvén waves in an inhomogeneous medium have found applications for heating of fusion plasma in the laboratory and heating of solar corona (for details see Uberoi[36] and the references therein). Another application of this theory is to understand the microscopic structures of aurora, which we shall discuss subsequently.

4.2. *Auroral dynamics*

Auroras are spectacular displays of luminuous radiation in the arctic skies. They occur simultaneously and symmetrically in both the polar regions, with their symmetry defined by the Earth's magnetic field. The northern aurora is known as Aurora Borealis (Northern Dawn) and the southern as Aurora Australis (Southern Dawn). From the ground, aurora appears to be a curtain of light streaked with rays. The curtain begins at an altitude of several hundred kilometers and ends at about 100 km above the ground. It shows shimmering undulations. Aurora is always seen to ebb and flow across the polar sky. This shows that aurora is dynamic and with the understanding of the space environment of the Earth it is now known that aurora is a part of the overall interactions of the solar wind, the Earth's magnetosphere and the Earth's atmosphere[37]. The magnetic nature of the aurora can be seen clearly from outer space. Centred on each of the geomagnetic poles is a great luminous oval that is a permanent feature of the planet. Auroras occur virtually every night in auroral ovals around both the magnetic poles.

Auroras are produced by electrons and protons from the magnetotail and the outer Van Allen belt striking the upper atmosphere. When oxygen and nitrogen atoms are hit by energetic particles, they are excited or ionized. Then they give off light at characteristic wavelengths as they return to their ground states. Blue and red emissions from nitrogen atoms struck by electrons with energies of a few thousand electron volts are sometimes seen at an altitude of about 110 km. The more typical green colour of fast-moving auroral rays comes from excited oxygen atoms between 110 and 250 km up. A rather steady red glow some 300–400 km in altitude is produced by oxygen atoms struck by less energetic particles. Our atmosphere thus acts like a television screen recording the 'images' imposed upon in by magnetospheric processes.

The overall dynamics of the aurora is now understood to be obviously governed by the macroscopic dynamics of the magnetosphere geomagnetic tail configuration. But auroras reveal very clear microscopic patterns such as the discrete arcs that have certain shapes with spacings of a few tens of kilometers. Hasegawa[38] suggested that the

filamentary structures existing within the diffuse aurora can be explained by considering the microscopic effects in the macroscopic MHD theory of Alfvén waves in inhomogeneous plasmas.

4.3. Kinetic effects

The microscopic scale in the magnetosphere can be defined as a scale comparable to or shorter than the ion gyroradius. A consideration of the finite Larmor radius effects in the MHD equation for uniform plasmas gives the following dispersion relation for the Alfvén wave:

$$\omega^2 = k_\parallel^2 V_A^2 \left(1 + k_\perp^2 \rho^2\right), \tag{20}$$

where $k_\parallel$ is wave number along the magnetic field lines and $k_\perp$ in the transverse direction and

$$\rho = \left[\frac{3}{4} + (T_e / T_i)\right] \rho_i^2, \tag{21}$$

ρ_i being the ion Larmor radius. T_e and T_i are the electron and ion temperatures. The Alfvén wave defined by (20) is called the kinetic Alfvén wave (KAW). It is noted from (20) that when $\rho_i \to 0$ the dispersion equation gives that Alfvén wave. Further, it is necessary to point out that eqn (20) is obtained when $m_e / m_i < \beta < 1$, where β is the plasma parameter giving the ratio of plasma to magnetic pressure.

The kinetic effects are important when the perpendicular wavelength $k_\perp$ is comparable to the ion gyroradius. Because of the coupling to the electrostatic perturbation, the kinetic Alfvén wave accompanies a parallel electric field $E_\parallel$ in addition to the perpendicular electric fields, given by

$$\left(\frac{k_\perp}{E_\perp}\right)\left(\frac{E_\parallel}{k_\parallel}\right) \sim k_\perp^2 \rho_i^2 \quad \text{when } T_e \approx T_i.$$

From (1) we see that this wave will propagate in the nonuniform medium when $k_\parallel^2 V_A^2(x) < \omega^2$, as $k_\perp^2 > 0$, i.e., it propagates on the higher density side. Also, due to coupling to ion-acoustic wave kinetic Alfvén wave can undergo collisionless Landau damping. Unlike MHD Alfvén wave, the kinetic Alfvén wave can propagate across the magnetic field.

In case $\beta < m_e / m_i \ll 1$, the Alfvén wave couples also to plasma oscillations as the electron inertial terms are finite. In this case the dispersion relation (20) becomes

$$\omega^2 = k_\parallel^2 v_A^2 \left(1 + \frac{3}{4} k_\perp^2 \rho_i^2\right)\left[1 + \frac{k_\perp^2 c^2}{\omega_{pe}^2}\right]^{-1}. \tag{22}$$

In the latter case it propagates towards decreasing density in nonuniform plasma.

Though the kinetic-theoretical model of plasmas retains the finite Larmor radius effects fully, the kinetic approach is highly cumbersome. There are studies of kinetic effects on Alfvén waves by using the Hall–MHD model[39–41] and the two-fluid model[42]. More recently, a generalized Hall–MHD model, taking full account of the electron inertia terms, has been considered by Uberoi and Das[43]. They find that the hydromagnetic wave dispersion relation for generalized Ohm's law and MHD equations is

$$\omega^6 - \omega^4 \left[\frac{1}{\alpha} + \frac{X}{\alpha^2} + \frac{1}{\alpha \cos^2\theta} + \frac{\beta}{\cos v_\theta} \right] + \frac{\omega^2}{\alpha^2 \cos^2\theta} \left[1 + (2\alpha + X)\beta \right] - \frac{\beta}{\alpha^2 \cos^2\theta} = 0, \quad (23)$$

where

$$\omega \equiv \frac{\omega}{kV_A \cos\theta}, \quad \alpha = \left(1 + \frac{k^2 \rho_s^2}{\beta} \frac{m_e}{m_i} \right), \quad X = \frac{k^2 \rho_s^2}{\beta}, \quad \beta = \frac{S^2}{V_A^2}, \rho_s = \frac{s}{\omega_\omega} > \rho_i.$$

In the limit $\cos^2\theta \ll \beta < 1$, eqn (23) can be written as

$$\omega^4 \left(\frac{1}{\alpha} + \beta \right) - \frac{\omega^2}{\alpha^2} \left(1 + 2\alpha\beta + k_\perp^2 \rho_s^2 \right) + \frac{\beta}{\alpha^2} = 0. \quad (24)$$

Equation (24) gives the dispersion relation for the kinetic Alfvén wave as (20) when $\alpha = 1$ and as (22) when $\alpha \neq 1$. This limiting case was also discussed by Belmont[41].
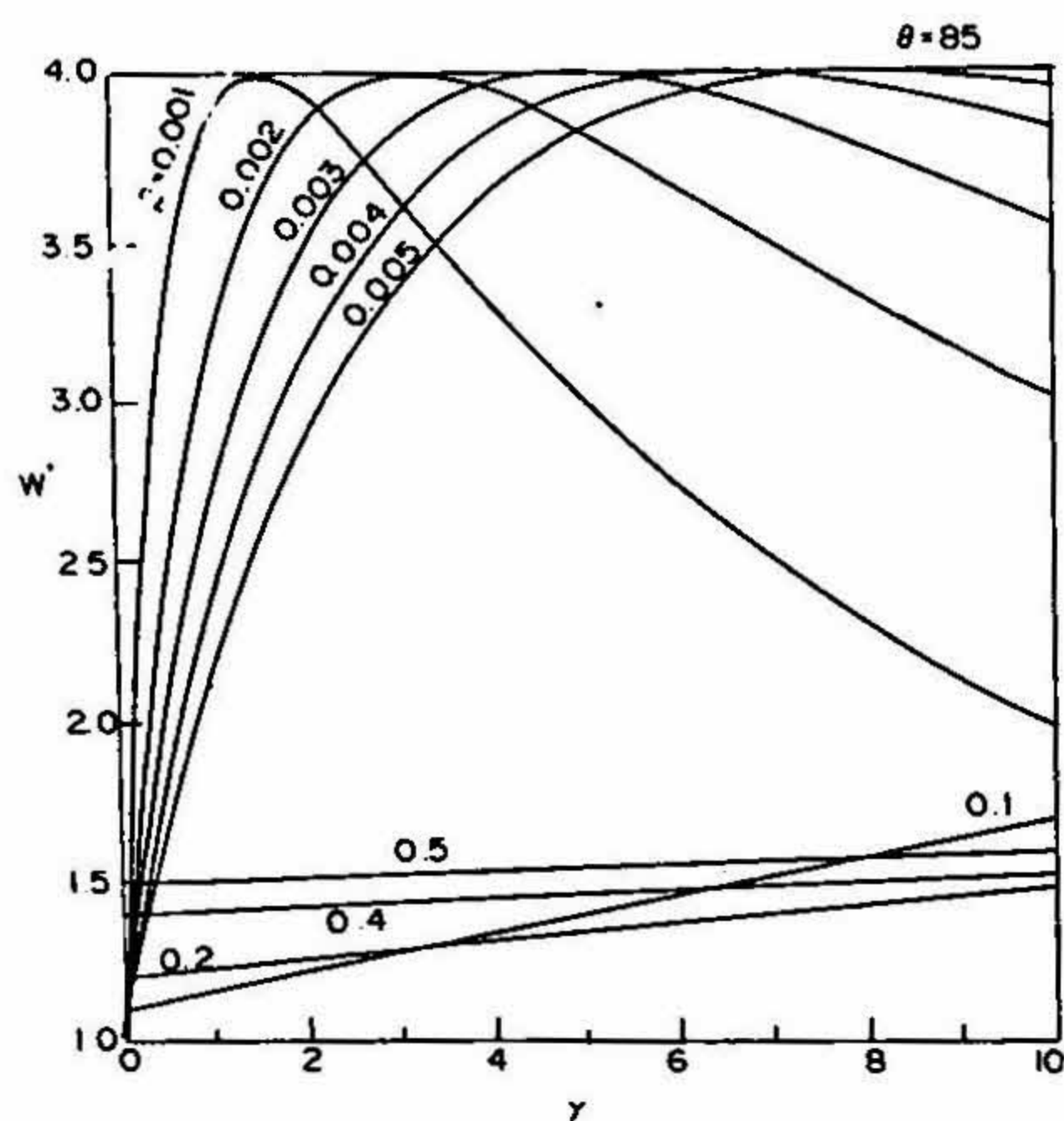

FIG. 10. Variation of $W \equiv \left[\dfrac{\omega}{kV_A \cos\theta} \right]^2$ with $\gamma = k_\perp^2 \rho_s^2$ for different values of β and $\theta = 85°$ considering the generalized Hall–MHD treatment to study the kinetic effects on the Alfvén waves.

In general, not including angles $\theta = 0$ and $\pi/2$, which appear to be special cases, we note from the dispersion curves the following (Fig. 10):

(i) when electron inertial effects are important or $\beta < m_e/m_i$ the dispersion curves for all θ show curvatures which change, thus making the parallel phase velocity sub- or super-Alfvénic.

(ii) the curves are very sensitive to the value of the angle of propagation and differ considerably in cases of $\beta > m_e/m_i$ and $\beta < m_e/m_i$.

A very appealing mechanism which allows MHD waves to modulate or precipitate the free electrons is heating or acceleration of electrons directly by the kinetic Alfvén wave. When the scale size of the resonance region approaches the electron inertia length or the ion gyroradius, then linear mode conversion to KAW can occur. This process has an advantage, as only mode conversion to the KAW need take place and the energy transfer is directly from the MHD to the microscopic regime through the heating of particles.

The characteristic properties of the acceleration of particles by the kinetic Alfvén wave along the line of force show that the acceleration occurs on this magnetic flux surfaces separated by a distance of $2\pi\rho_i$ as $k_x \sim 1/\rho_i$ and these flux surfaces have a wave pattern (east-west direction) with the wavelength $\sim 1/k_y$. Also, the acceleration pattern is time-dependent. These properties strongly suggest that there are possible connections between the phenomena of MHD field line resonances and discrete auroral arc, which have generated considerable interest in the understanding of KAW heating mechanism and formation of aurora[43].

The understanding of the kinetic effects and mode conversion to the kinetic Alfvén wave, however, needs some further considerations. Firstly, the kinetic Alfvén wave may not exist in the presence of collisional effects like conductivity. A careful study must be done to determine the ionospheric losses on the widths of the resonance regions and the formation of the kinetic Alfvén waves, especially when looking at auroral arc formation[43]. The generalized Hall–MHD treatment shows that the kinetic Alfvén wave is a limiting case of angle θ such that $\cos^2 \theta \ll \beta < 1$. Therefore, a full treatment of the study of mode conversion by retaining all the modes of propagation as in dispersion relation (23) is required to understand the angle effect on the resonant mode coupling and absorption of Alfvén waves in the situation when kinetic effects are important.

5. Conclusion

The phenomena of whistlers, ULF wave or micropulsations and aurora are now known to occur in the planetary magnetospheres of our solar system[44,45]. The mathematical studies of plasma waves discussed here can find application in understanding the space environment of other planets.

References

1. STOREY, L. R. O. *Phil. Trans. R. Soc. Lond. A*, 1953, **246**, 113–141.

2. STIX, T. H. *The theory of plasma waves*, 1962, p. 9, McGraw-Hill.

3. UBEROI, C.   *J. Math. Phys. Sci.*, 1972, **6**, 303–314.

4. GURNETT, D. A., SHAWHAN, S. D.,   *J. Geophys. Res.*, 1965, **70**, 1665–1688.
   BRICE, N. M. AND SMITH, R. L.

5. BUDDEN, K. G.   *Radio waves in ionosphere*, Ch. 6, 1961, Cambridge University Press.

6. UBEROI, C. AND DAS, G. C.   *Plasma Phys.*, 1973, **16**, 669–676.

7. SHAWHAN, S. D.   *J. Geophys. Res.*, 1966, **71**, 5585–5598.

8. DAS, G. C. AND UBEROI, C.   *J. Geophys. Res.*, 1972, **77**, 5597–5601.

9. UBEROI, C.   *Phys. Fluids*, 1973, **16**, 704–705.

10. DUNGEY, J. W.   *Phil. Mag.*, 1953, **44**, 725–738.

11. UBEROI, C.   *Indian J. Pure Appl. Phys.*, 1964, **2**, 13; *Phys. Fluids*, 1972, **15**,
                                              1673–1675.

12. UBEROI, C.   Alfvén waves in magnetospheric plasma: Micropulsation and particle
                                              acceleration, Invited Review talk, *Proc. Int. Workshop on Alfvén
                                              Waves*, Rio de Janeiro, Brazil, Nov. 1994.

13. HASEGAWA, A. AND UBEROI, C.   *The Alfvén wave*, 1982, Tech. Information Centre, US Department of
                                              Energy, Springfield, Virginia, 22161.

14. YUMOTO, K. AND SAITO, T.   *J. Geophys. Res.*, 1982, **87**, 5159–5182.

15. UBEROI, C.   *J. Geophys. Res.*, 1983, **88**, 4959.

16. UBEROI, C.   *J. Geophys. Res.*, 1989, **94**, 6941–6944.

17. UBEROI, C.   *J. Plasma Phys.*, 1994, **52**, 215–221.

18. UBEROI, C., LANZEROTTI, L. J.   to be published.
    AND WOLFE, A.

19. HASEGAWA, A., TSUI, H. K.   *Geophys. Res. Lett.*, 1983, **10**, 765–767.
    AND ASSIS, A. S.

20. KIVELSON, M. G. AND   *J. Geophys. Res.*, 1986, **91**, 4345–4351, *Geophys. Res. Lett.*, 1985,
                                              12, 49–52.
    SOUTHWOOD, D. J.

21. UBEROI, C.   *J. Geophys. Res.*, 1989, **94**, 2745–2746.

22. ALLAN, W., WHITE, S. P.   *Planet Sp. Sci.*, 1986, **31**, 371–385.
    AND POULTER, E. M.

23. INHESTER, B.   *J. Geophys. Res.*, 1987, **92**, 4751–4756.

24. ZHU, X. AND KIVELSON, M. G.   *J. Geophys. Res.*, 1989, **94**, 1479–1485.

25. LEE, D. H. AND LYSAK, R. L.   *J. Geophys. Res.*, 1989, **94**, 17097–17103.

26. SAMSON, J. C., HARROLD, B. G.,   *Geophys. Res. Lett.*, 1992, **19**, 441–444.
    RUOHONIEMI, J. M.,
    GREENWALD, R. A. AND
    WALKER, A. D. M.

27. WRIGHT, A. N.   *J. Geophys. Res.*, 1994, **99**, 159–167.

28. HARROLD, B. G. AND   *Geophys. Res. Lett.*, 1992, **19**, 1811–1814.
    SAMSON, J. C.

29. UBEROI, C.   *J. Geophys. Res.*, 1988, **93**, 295–298.

30. UBEROI, C. AND SEDLACEK, Z.   *Phys. Fluids*, 1992, **134**, 6-8.

31. UBEROI, C.   *J. Geophys. Res.*, 1995, **100**(A7), 12127-12131.

32. RADOSKI, H. R.   *J. Geophys. Res.*, 1974, **79**, 595-603.

33. BAUMJOHANN, W., JUNGINGER, H.,   *J. Geophys. Res.*, 1984, **89**, 2765-2769.
    HARENDEL, G. AND BAUER, O. H.

34. LAU, Y. Y.   *Phys. Rev. Lett.*, 1979, **42**, 779-781.

b. LAU, Y. Y., DAVIDSON, R. C.   *Phys. Fluids*, 1980, **23**, 1827-1831.
   AND HUI, B.

35. UBEROI, C.   *J. Geophys. Res.*, 1988, **93**, 7595-7597.

36. UBEROI, C.   Alfvén surface waves. In *Contemporary plasma physics* (Sodha, M. S., Tiwari, D. P. and Subbarao, D., eds), p. 43, McMillan India.

37. LANZEROTTI, L. J. AND   *Sky Telescope*, 1988, **76**, 360-362.
    UBEROI, C.

38. HASEGAWA, A.   *J. Geophys. Res.*, 1976, **81**, 5083-5090.

39. SOUTHWOOD, D. J. AND   *Space Sci. Rev.*, 1983, **35**, 301-366.
    HUGHES, W. J.

40. CAO, F. AND KAN, J. R.   *J. Geophys. Res.*, 1987, **92**, 3397-3401.

41. GOERTZ, C. K. AND   *J. Geophys. Res.*, 1979, **84**, 7239-7246.
    BOSWELL, R. W.

42. BELMONT, G. AND REZEAU, L.   *Annls Geophys. A*, 1987, **5**, 59-69.

43. UBEROI, C. AND DAS, G. C.   *Proc. Int. Union of Geodesy and Geophysics, XXI General Assembly, Boulder, Colorado July 2-14, 1995*.

44. LANZEROTTI, L. J. AND   *Sky Telescope*, 1989, **77**, 149-152.
    UBEROI, C.

45. UBEROI, C.   *Earth's proximal space*, 1994, p. 101, Interline Publishing, Bangalore, India.